

Coralloite, $\text{Mn}^{2+}\text{Mn}^{3+}(\text{AsO}_4)_2(\text{OH})_2 \cdot 4\text{H}_2\text{O}$, a new mixed valence Mn hydrate arsenate: Crystal structure and relationships with bermanite and whitmoreite mineral groups

ATHOS MARIA CALLEGARI,^{1,*} MASSIMO BOIOCCHI,² MARCO E. CIRIOTTI,³ AND CORRADO BALESTRA⁴

¹Dipartimento di Scienze della Terra e dell'Ambiente, Università degli Studi di Pavia, via Ferrata 1, I-27100 Pavia, Italy

²Centro Grandi Strumenti, Università degli Studi di Pavia, via Bassi 21, I-27100 Pavia, Italy

³Associazione Micromineralogica Italiana, via San Pietro 55, I-10073 Devesi-Ciriè, Italy

⁴Associazione Micromineralogica Italiana, via Delfino 74, I-17017 Millesimo, Italy

ABSTRACT

Coralloite is a new mineral found at the Monte Nero Mine (Rocchetta Vara, La Spezia, Liguria, Italy) having the simplified formula $\text{Mn}^{2+}\text{Mn}^{3+}(\text{AsO}_4)_2(\text{OH})_2 \cdot 4\text{H}_2\text{O}$. It occurs as sub-millimetric lamellar cinnabar-red crystals elongated on [100] and flattened on (001), isolated or forming wisps up to 0.5–1 mm long. Associated phases are calcite, inesite, quartz, brandtite, sarkinite, and tilasite in a chert matrix.

Crystals are pleochroic, yellow along [100] and orange-red in directions normal to it. Extinction is parallel to the cleavage traces and elongation is negative. The small crystal size does not allow accurate determination of refraction indices. Crossed polar observations of crystals placed in diiodomethane ($n = 1.74$) suggest that the mean refractive index is close to that value.

Coralloite is triclinic, space group $P1$, $a = 5.5828(7)$, $b = 9.7660(13)$, $c = 5.5455(7)$ Å, $\alpha = 94.467(3)$, $\beta = 111.348(2)$, $\gamma = 93.850(2)^\circ$, $V = 279.26(6)$ Å³, $Z = 1$. The five strongest lines in the simulated powder diffraction pattern (d_{obs} , l , hkl) are: 9.710 Å, 100.0, (0 $\bar{1}$ 0), 5.166 Å, 77.1, (100); 5.136 Å, 79.7, (001); 3.342 Å, 64.8, ($\bar{1}$ 21); 3.324 Å, 33.6, (1 $\bar{2}$ 1).

The structure of coralloite (final R_{all} 0.044 for 3092 observed reflections) shows similarities with bermanite: $\text{Mn}^{2+}\text{Mn}^{3+}(\text{PO}_4)_2(\text{OH})_2 \cdot 4\text{H}_2\text{O}$ and ercittite: $\text{Na}_2\text{Mn}^{3+}(\text{PO}_4)_2(\text{OH})_2 \cdot 4\text{H}_2\text{O}$. In particular, these three minerals exhibit the same structural slab formed by $[\text{Mn}^{3+}(\text{XO}_4)_2(\text{OH})_2]$; X = As or P. However, these structural slabs are connected by interposed layers of different polyhedra for each mineral species.

Keywords: Coralloite, bermanite, arsenates, structure refinement, Monte Nero area, Liguria

INTRODUCTION

Eastern Liguria is characterized by the presence of manganese ores located near the base of chert sequences overlaying Jurassic ophiolites of the Northern Apennines. The area is comprised between the Graveglia and Bargonasco valleys and defines the “Gambatesa district” from the name of the most famous mine in this zone. Other minor manganese deposits are located near La Spezia (Cerchiara and Monte Nero mines). In particular, the Monte Nero area is a portion of the “External Liguride Units.” Ophiolites are the most common rocks; subordinated gabbros and ophiolitic breccias (ophicalcites) also occur; these rocks are dated to the Late Jurassic period. The sedimentary rocks that overlay ophiolites are prevailing cherts. This area is very interesting for the presence of several Mn-bearing minerals together with abundant secondary phases. A complete description of these Mn-ores is presented in Cabella et al. (1998) and references therein. Red, tiny wisps of a secondary phase found in this zone, similar to other mineral species belonging to this area [e.g., geigerite (Cabella et al. 2000; Palenzona et al. 2002), reppiaite (Basso et al. 1992), sarkinite (Cortesogno et al. 1979)] have been studied combining single-crystal X-ray diffraction experiment together with electron microprobe analyses. This study allowed us to

identify the red crystals as the new mineral species coralloite and its complete description is reported here. The mineral name has been assigned in honor of Giorgio Corallo (b. 1937), a keen mineral collector, who first found several new minerals in this area, as cassagnaites (Basso et al. 2008; Palenzona and Martinelli 2009), gravegliaite (Basso et al. 1991), and reppiaite (Basso et al. 1992). He is considered “teacher” and “tutor” of several Ligurian mineralogical collectors.

The new mineral and its name were approved by the Commission on New Minerals Nomenclature and Classification IMA 2010-012 (Callegari et al. 2010). Type material (the selected crystal used for X-ray diffraction study and the residual sample) has been deposited at the Museo di Mineralogia, Dipartimento di Scienze della Terra, Università degli Studi di Pavia, Italy, with catalog number 2010-001.

OCCURRENCE AND PARAGENESIS

In Eastern Liguria, manganese ores occur as stratiform layers (0.01–0.10 m thick) or massive lenses (5–20 m thick) formed by Mn-oxides fractionation from hydrothermally metal-bearing siliceous muds during turbiditic re-sedimentation. The resulting Mn-bearing ores consist of rhythmic interlaying of braunite-bearing levels (5–15 cm thick) and hematite-rich cherts. All the sequences of tectono-metamorphic events that favored the

* E-mail: athosmaria.callegari@unipv.it

formations of Mn layers or Mn lenses, as well as the chemical processes that developed Mn-silicate and Mn carbonates, are described in Cabella et al. (1998) and references therein.

Coralloite is a new secondary mineral that occurs in thin manganese stratiform ores at Monte Nero (Rocchetta Vara, La Spezia, Liguria, Italy); the ores are located near the base of a chert sequence named "Diaspri di Monte Alpe" formation that overlays Jurassic ophiolites of the Bracco unit. In particular, coralloite has been found in an abandoned manganese mine. The host matrix of coralloite crystals is a chert with associated several secondary minerals as calcite, inesite, quartz, brandtite, sarkinite, and tilasite.

For decades it has been quite difficult to find minerals at the Monte Nero manganese mine. As a matter of fact, the main dumps were removed and the galleries were buried during the environmental reclamation of the area. However, about 15 years ago and for a short time, several tons of chert were extracted from the Monte Nero mine by building industry. These works brought to light some matrices richly mineralized with esthetic inesite and several copper secondary minerals (mainly cuprite and olivenite). Few specimens with rare manganese species like geigerite, sarkinite, and brandtite were also found in a matrix of Mn-oxides intergrowing with a hard yellowish chert. The first red, tiny wisp of coralloite crystals was found by grinding one of the above cited specimens rich of internal microvugs mainly mineralized with sarkinite and brandtite; an additional occurrence of coralloite was reported as few grains on Mn-oxides, strictly associated with tilasite.

The genesis of coralloite should be the same of the other rare As-Mn minerals found in this area. In particular, the formation of these secondary phases was related to the presence of important amounts of As and Mn in fluids circulating in the system of veins during the final tectono-metamorphic processes occurring at Monte Nero manganese deposits. It is well known that the circulation of these fluids allowed the concentration of dispersed elements (such as Ba, Sr, As, V, B, and Li) and the genesis of rare and new secondary minerals in this area (Viviani 1807; Issel 1892; Mogno 1924; Bonatti et al. 1976; Antofilli et al. 1983; Boni 1986; Guelfi and Orlandi 1987; Cabella et al. 1998, 2000; Marroni et al. 2002; Garuti et al. 2008; Marchesini and Palenzona 1997; Marchesini 1999; Palenzona et al. 2002; Balestra et al. 2009; Bersani et al. 2009; Passarino 2009).

After approval by IMA-CNMNC of the new coralloite mineral species from Monte Nero (Italy), previously collected but unidentified mineral species from two Swiss localities (Falotta and Alpe Tanatz) have been recognized as coralloite, on the basis of the crystal morphology, qualitative SEM-EDS analysis and powder diffraction pattern (Roth and Meisser 2011).

EXPERIMENTAL METHODS

X-ray diffraction analysis and structure refinement

A small single crystal was selected for X-ray data collection performed on a Bruker-AXS diffractometer equipped with the SMART-APEX CCD detector. Data collection was carried out with operating conditions 50 kV and 30 mA and graphite-monochromatized MoK α radiation ($\lambda = 0.71073$ Å). Omega rotation frames (scan width 0.3°, acquisition time 30 s, sample-to-detector distance 5 cm) were processed with the SAINT software suite (Bruker 2003) for data reduction, including intensity integration, background, and Lorentz-polarization

corrections, and for the measure of final unit-cell parameters. Absorption effects were evaluated by an empirical method (SADABS software, Sheldrick 1996) and absorption correction was applied to the data. Details on data collection are reported in Table 1.

The crystal structure was solved by direct methods (SIR97; Altomare et al. 1999) and refined in the space group *P1*. Reflections with $I_o > 3\sigma(I_o)$ were considered as observed during the unweighted full-matrix least-squares refinement on *F* done using a locally modified version of ORFLS (Busing et al. 1962). Neutral scattering curves were used for all atom sites and site populations were fixed to 1, assuming absence of isomorphous substitutions. Atom coordinates, site population and isotropic displacement parameters are listed in Table 2; selected bond distances and angles in Table 3 and anisotropic displacement parameters in Table 4. A table listing the observed and calculated structure factors (Table 5¹) has been deposited, along with the CIF¹.

Coralloite contains 2 OH groups and 4 water molecules but the final ΔF map was unable to establish positions for H atoms. Assignment of O-sites belonging to OH and water species was assumed on the basis of crystal-chemical evidences (mono-coordinated O-sites are anions of water molecules, two-coordinated O-sites not linked to tetrahedral species are anions of OH group), and this assignment is fully confirmed by the final bond-valence analysis (Table 6).

No sufficient amount of material suitable for powder diffraction study was available. A complete X-ray powder diffraction pattern (Table 7) was simulated (for CuK α radiation) combining the integrated intensities from the single-crystal diffraction study at the proper 2θ values, and taking multiplicities and *Lp* factors into account (XPREP program of the SAINT software suite, Bruker 2003).

Chemical composition

A preliminary qualitative SEM-EDS analysis provided a list of chemical elements present in the sample. It resulted solely constituted by Mn, As, and O. Only a point analysis detected a trace amount of P and F. The presence of F was attributed to an accidental contamination of the sample and the presence of P to trace impurity of the material.

A subsequent quantitative SEM-WDS analysis was carried out using an electron microprobe (Zeiss Supra 50VB working at 16 kV, 1.5 nA, 1–10 μ m beam diameter) on a wispy coralloite aggregate (Fig. 1), selecting a flat portion of

¹ Deposit item AM-12-017, CIF and Table 5. Deposit items are available two ways: For a paper copy contact the Business Office of the Mineralogical Society of America (see inside front cover of recent issue) for price information. For an electronic copy visit the MSA web site at <http://www.minsocam.org>, go to the American Mineralogist Contents, find the table of contents for the specific volume/issue wanted, and then click on the deposit link there.

TABLE 1. Crystal data for coralloite

Crystal size (mm)	0.07 × 0.04 × 0.03
<i>a</i> (Å)	5.5828(7)
<i>b</i> (Å)	9.7660(7)
<i>c</i> (Å)	5.5455(13)
α (°)	94.467(2)
β (°)	111.348(3)
γ (°)	93.850(2)
<i>V</i> (Å ³)	279.26(8)
<i>Z</i>	1
Space group	<i>P1</i>
Detector type	CCD plate
Wavelength (Å)	0.71073
μ MoK α (cm ⁻¹)	91.6
No. collected <i>F</i>	4874
No. unique <i>F</i>	3092
<i>R</i> _{sym} merging identical indices only	0.022
Completeness	99.9
Mean redundancy	1.6
No. Obs. <i>F</i> [$ I/\sigma(I) \geq 3$]	2641
2θ range (°)	4–60
<i>h</i> range	$\bar{7}$ →7
<i>k</i> range	$\bar{13}$ →13
<i>l</i> range	$\bar{7}$ →7
<i>F</i> (000)	263
Largest diff. peak/hole (eÅ ⁻³)	-0.795/1.126
Flack's parameter	0.058 (18)
No. parameters refined	191
<i>R</i> _{obs}	0.037
<i>R</i> _{int}	0.044

TABLE 2. Atom site populations, fractional atom coordinates, and isotropic displacement parameters $U_{eq} \times 10^4 \text{ \AA}^2$, (estimated standard deviations in parentheses)

Site	Site population	x/a	y/b	z/c	U_{eq}
As1	As ⁵⁺	0.0643(4)	0.1933(2)	0.5121(4)	109(3)
As2	As ⁵⁺	-0.0661(4)	0.8037(2)	0.4850(4)	121(3)
M1	Mn ³⁺	0	0	0	113(3)
M2	Mn ³⁺	0.5006(5)	0.0047(3)	0.4997(5)	107(3)
M3	Mn ²⁺	0.1697(4)	0.5046(2)	0.3445(4)	167(4)
O1	O ²⁻	-0.0734(13)	0.1508(7)	0.1866(13)	114(21)
O2	O ²⁻	0.0608(14)	0.8431(8)	0.8124(14)	160(24)
O3	O ²⁻	-0.1079(14)	0.1081(8)	0.6569(14)	166(25)
O4	O ²⁻	0.1118(13)	0.8912(7)	0.3496(14)	146(24)
O5	O ²⁻	0.3748(14)	0.1571(7)	0.6328(15)	164(24)
O6	O ²⁻	0.6282(13)	0.8512(7)	0.3668(13)	125(21)
O7	O ²⁻	0.0459(13)	0.3631(6)	0.5591(14)	165(21)
O8	O ²⁻	-0.0853(12)	0.6376(8)	0.4180(15)	208(23)
OH1	OH	0.3683(12)	0.0667(7)	0.1556(13)	123(21)
OH2	OH	0.6237(13)	0.9414(7)	-0.1536(14)	130(21)
OW1	H ₂ O	0.4615(15)	0.3745(8)	0.2708(19)	348(31)
OW2	H ₂ O	0.2816(11)	0.6416(6)	0.1007(12)	187(19)
OW3	H ₂ O	-0.1225(12)	0.4105(7)	-0.0471(13)	241(22)
OW4	H ₂ O	0.4961(15)	0.6011(9)	0.7240(17)	349(29)

TABLE 3. Selected bond distances (Å) and angles (°) for coralloite

As1-O1	1.689(7)	M2-O3 ¹	2.176(7)	O1-As1-O3	109.2(3)
As1-O3	1.679(7)	M2-O4 ⁵	2.203(7)	O1-As1-O5	111.9(3)
As1-O5	1.689(7)	M2-O5	1.897(7)	O1-As1-O7	105.4(3)
As1-O7	1.674(6)	M2-O6 ⁵	1.911(7)	O3-As1-O5	109.9(3)
	1.683	M2-OH1	1.941(7)	O3-As1-O7	109.4(3)
As2-O2	1.692(7)	M2-OH2 ²	1.957(7)	O5-As1-O7	110.8(3)
As2-O4	1.677(7)		2.014		
As2-O6 ²	1.702(6)			O2-As2-O4	109.7(3)
As2-O8	1.623(7)	M3-O7	2.128(6)	O2-As2-O6	109.2(3)
	1.673	M3-O8	2.114(6)	O2-As2-O8	108.9(4)
M1-O1	1.887(6)	M3-OW1	2.262(8)	O4-As2-O6	108.3(3)
M1-O2 ³	1.904(7)	M3-OW2	2.189(6)	O4-As2-O8	113.0(3)
M1-O3 ⁴	2.159(7)	M3-OW3	2.265(7)	O6-As2-O8	107.6(3)
M1-O4 ⁵	2.192(7)	M3-OW4	2.304(8)		
M1-OH1	1.959(7)		2.210		
M1-OH2 ⁶	1.981(7)				
	2.014				
O1-M1-O2	177.4(4)	O5-M2-O6	179.8(4)	OW1-M3-O8	176.2(3)
O1-M1-OH1	89.6(3)	O5-M2-OH1	89.8(3)	OW4-M3-OW3	174.4(3)
O1-M1-OH2	87.9(3)	O5-M2-OH2	89.4(3)	OW4-M3-O8	90.0(3)
O2-M1-OH1	92.7(3)	O6-M2-OH1	90.3(3)	OW4-M3-OW1	87.5(3)
O2-M1-OH2	89.9(3)	O6-M2-OH2	90.4(3)	OW3-M3-O8	94.0(2)
OH1-M1-OH2	177.3(3)	OH1-M2-OH2	178.3(3)	OW3-M3-OW1	88.2(3)

Note: Symmetry codes: ¹ x+1, y, z; ² x-1, y, z; ³ x, y-1, z-1; ⁴ x, y, z-1; ⁵ x, y-1, z; ⁶ x-1, y-1, z; ⁷ x, y-1, z+1.

TABLE 4. Anisotropic atom-displacement coefficients (U_{ij} , Å² × 10⁴) in coralloite; the atom-displacement parameter is of the form: $\exp[-2\pi^2(h^2a^{*2}U_{11} + k^2b^{*2}U_{22} + l^2c^{*2}U_{33} + 2hka^*b^*U_{12} + 2hla^*c^*U_{13} + 2klb^*c^*U_{23})]$

Site	U_{11}	U_{22}	U_{33}	U_{12}	U_{13}	U_{23}
As1	100(4)	126(4)	120(5)	29(3)	61(4)	14(4)
As2	100(4)	138(4)	141(5)	29(3)	64(4)	12(4)
M1	84(4)	146(4)	117(4)	34(3)	44(3)	10(3)
M2	81(4)	143(4)	107(4)	37(3)	42(3)	9(3)
M3	175(5)	165(5)	193(6)	33(4)	104(5)	22(4)
O1	133(30)	119(29)	84(31)	78(24)	26(25)	-2(24)
O2	128(31)	242(36)	141(35)	66(27)	77(28)	31(29)
O3	138(35)	223(37)	147(36)	-39(28)	80(30)	4(29)
O4	100(32)	172(34)	190(37)	4(26)	80(29)	39(28)
O5	153(35)	156(32)	176(36)	47(26)	54(29)	-12(27)
O6	53(28)	205(31)	101(33)	50(23)	12(25)	-31(26)
O7	261(30)	83(28)	222(33)	25(23)	160(26)	82(25)
O8	83(24)	225(35)	301(39)	40(23)	61(25)	-30(29)
OH1	78(30)	207(32)	99(31)	15(24)	58(25)	-15(24)
OH2	77(29)	188(31)	136(33)	32(24)	42(26)	58(25)
OW1	307(37)	383(43)	492(53)	150(33)	259(38)	208(38)
OW2	170(27)	204(28)	179(28)	29(22)	53(22)	28(22)
OW3	220(30)	241(30)	281(34)	21(24)	131(27)	-48(25)
OW4	298(40)	409(43)	313(44)	-36(34)	103(35)	-12(35)

TABLE 6. Bond-valence analysis (v.u.) of coralloite

Site charge	5+	5+	3+	3+	2+
Atom site	As1	As2	M1	M2	M3
O1	1.24		0.71		1.95
O2		1.22	0.68		1.90
O3	1.27		0.34	0.32	1.93
O4		1.28	0.31	0.30	1.89
O5	1.23			0.69	1.92
O6		1.19		0.67	1.86
O7	1.29				0.40
O8		1.48			0.42
OH1			0.58	0.61	1.19
OH2			0.55	0.59	1.14
OW1					0.28
OW2					0.34
OW3					0.28
OW4					0.25
	5.03	5.17	3.17	3.18	1.97

Note: Calculated after Brown and Altermatt (1985) with the parameters given by Brese and O'Keeffe (1991).

TABLE 7. Complete simulated X-ray powder diffraction pattern (the intensities of the 10 strongest lines are marked in bold)

d (Å)	I_{rel}	hkl	d (Å)	I_{rel}	hkl
9.710	100.0	0 1 0	2.437	4.7	2 1 0
5.166	77.1	1 0 0	2.399	5.6	1 3 1
5.136	79.7	0 0 1	2.378	2.6	0 2 2
4.844	6.3	0 2 0	2.345	3.9	2 2 1
4.766	12.8	1 1 0	2.231	6.0	2 1 2
4.754	9.1	0 1 1	2.172	1.9	0 2 2
4.595	1.1	1 0 1	2.135	8.3	1 4 1
4.382	3.2	1 1 0	2.109	6.7	1 3 1
4.339	1.4	0 1 1	2.081	1.1	2 2 2
4.158	13.1	1 1 1	2.028	2.9	2 0 1
3.736	8.5	0 2 1	2.019	3.0	1 0 2
3.728	6.4	1 2 0	1.938	5.0	0 5 0
3.367	17.3	1 2 0	1.930	3.1	1 1 2
3.342	64.8	1 2 1	1.924	3.6	2 3 0
		0 2 1	1.879	2.2	2 3 2
3.324	33.6	1 2 1	1.866	2.3	2 4 1
3.229	2.5	0 3 0	1.821	2.5	2 3 1
3.113	5.3	1 0 1	1.799	4.9	3 1 1
2.878	20.3	0 3 1	1.770	7.6	1 2 3
2.873	22.0	1 3 0	1.729	4.7	3 1 2
2.855	19.6	1 1 1	1.728	6.2	3 1 0
	8.9	1 2 1	1.717	3.3	0 1 3
2.757	4.7	2 0 1	1.692	7.6	3 2 1
2.740	10.5	1 0 2	1.677	5.4	1 2 3
2.688	12.9	2 1 1	1.672	4.5	2 4 2
2.650	5.8	1 3 1	1.660	5.3	3 3 1
2.631	22.8	1 3 1	1.658	5.3	1 3 3
2.620	7.4	1 3 0	1.635	4.4	0 5 2
2.605	7.1	0 3 1	1.633	5.4	2 5 0
2.587	19.6	2 0 0	1.631	4.7	1 5 2
2.565	21.6	2 1 0	1.614	3.0	0 6 0
		0 0 2	1.588	1.0	1 6 0
2.551	16.8	0 1 2	1.568	5.6	2 1 2
2.453	11.6	1 2 2	1.556	3.8	2 0 2
2.450	9.0	2 2 1	1.545	2.4	1 3 3

a crystal normal to the gun direction. The standards used were Mn-metal for Mn and InAs alloy for As. Data reduction was done using the ZAF correction method.

The average of 3 analyses performed on a single grain gave the following wt%: MnO 38.55 ± 3.25, As₂O₃ 42.12 ± 0.94, tot 80.67. Afterward, the MnO and Mn₂O₃ ratio was recalculated to obtain electroneutrality, and water content was calculated to obtain 4 H₂O + 2 OH in the unit formula based on 14 anions, with 2 (OH) and 4 (H₂O) groups, as suggested by the crystallographic results.

The final chemical composition (wt%) results: Mn₂O₃ 28.61, MnO 12.84, As₂O₃ 42.12, H₂O 16.42, tot 99.99. The resulting empirical formula, normalized on 8 O²⁻ + 2 (OH)⁻ + 4 (H₂O) groups, was: Mn_{0.99}Mn_{1.99}As_{2.01}O₈(OH)₂(H₂O)₄. The simplified formula is Mn²⁺Mn³⁺(AsO₄)₂(OH)₂(H₂O)₄, which requires Mn₂O₃ 28.77, MnO 12.93, As₂O₃ 41.89, H₂O 16.41, total 100.00 wt%.

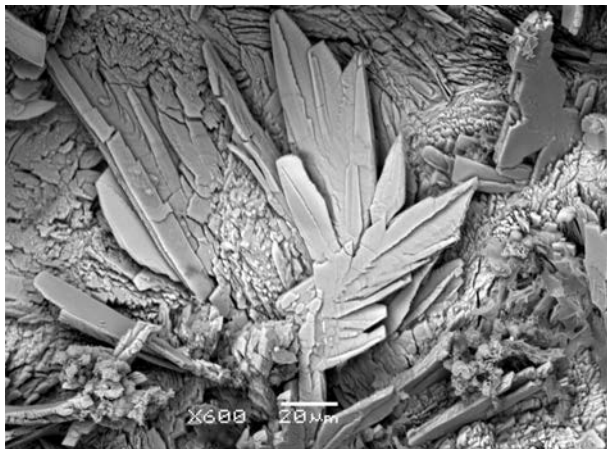


FIGURE 1. BSE micrograph showing a wisp of small coralloite crystals.

RESULTS

Discussion and structural relationships to the phosphate mineral bermanite

Coralloite is a very rare arsenate mineral that contains Mn^{2+} together with Mn^{3+} . As far as we know, the only two arsenate minerals that contain both divalent and trivalent manganese species are flinkite, $Mn_2^{2+}Mn^{3+}(AsO_4)(OH)_4$ (Kolitsch 2001), and jarosewichtite, $Mn_3^{2+}Mn^{3+}(AsO_4)(OH)_6$ (Dunn et al. 1982). However, these two minerals do not contain water molecules, whereas coralloite is the first arsenate hydrate mineral containing both Mn^{2+} and Mn^{3+} .

Coralloite shows close chemical analogies with the hydrated phosphate mineral bermanite (Hurlbut 1936; Hurlbut and Aristarain 1968). The unit formula for coralloite and bermanite is: $Mn^{2+}Mn_3^{3+}(AsO_4)_2(OH)_2 \cdot 4H_2O$ and $Mn^{2+}Mn_3^{3+}(PO_4)_2(OH)_2 \cdot 4H_2O$, respectively; thus evidencing that the two minerals differ for the homovalent exchange $P^{5+} \rightarrow As^{5+}$. However, these two minerals are not isomorphous (coralloite $P1$, bermanite $P2_1$) because only a portion of the crystal structure is identical.

Actually, the crystal structure of coralloite, as well as that of bermanite (Kampf and Moore 1976), is based on infinite chains of edge-sharing distorted $Mn^{3+}O_4(OH)_2$ octahedra. Each octahedron shares two O-OH edges with two adjacent octahedra. Each octahedron shares also all the four O vertexes with four isolated TO_4 tetrahedra ($T = As$ in coralloite and P in bermanite). Overall, four of the octahedral vertexes ($2OH + 2O$) are shared with two cation sites ($2 Mn^{3+}$ for OH , $1 Mn^{3+} + 1 T$ for O), whereas the remaining two O vertexes are shared among three cation sites ($2 Mn^{3+} + 1 T$). These connections yield a $[^{6}Mn_2^{3+}(OH)_2(^{4}TO_4)_2]$ slab ($T = As, P$), which is topologically identical in both minerals (Fig. 2). The octahedral Mn^{3+} chains extend along $[101]$ and the slabs are parallel to (010) ; these structural analogies are responsible for the similar values of a , c , and β between the two minerals: $a_{cor} = 5.583(1)$, $a_{ber} = 5.446(3)$ Å; $c_{cor} = 5.546(1)$, $c_{ber} = 5.428(3)$ Å; $\beta_{cor} = 111.35(1)$, $\beta_{ber} = 110.29(4)^\circ$.

In coralloite ($P1$) the Mn^{3+} octahedral cations are located in two independent crystallographic sites labeled M1 and M2, whereas in bermanite ($P2_1$) these two sites are symmetrically equivalent (M1; Kampf and Moore 1976). However, in both minerals Mn^{3+} octahedra exhibit a distorted octahedral coordination, with four equatorial M-(O,OH) distances (those corresponding to the twofold-coordinated anion sites) shorter than the other two

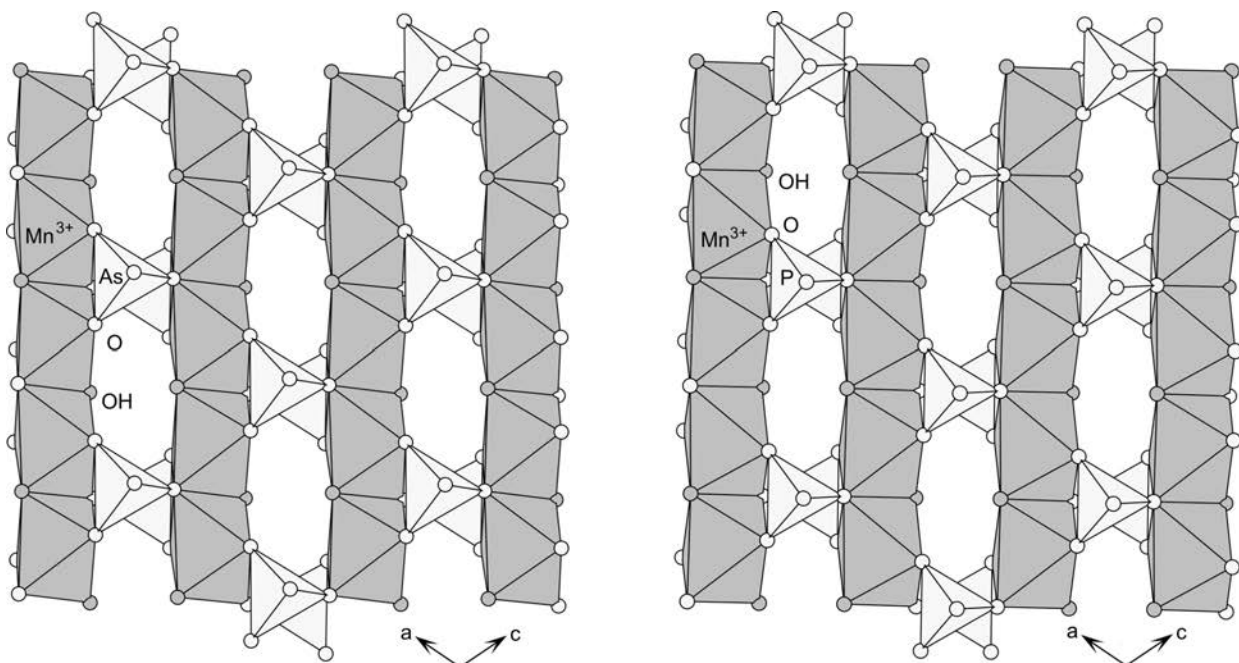


FIGURE 2. View down $[010]$ of the sheets formed by the $[^{6}Mn_2^{3+}(OH)_2(^{4}XO_4)_2]$ structural unit in coralloite ($X = As$, left) and bermanite ($X = P$, right).

apical M-O bonds (involving the threefold-coordinated anion sites): in coralloite the mean equatorial M-(O,OH) bond values are 1.993(7) Å for M1 and 1.927(7) for M2; the mean apical M-O bond values are 2.176(7) Å for M1 and 2.190(7) Å for M2. This [4+2]-coordination is suitable to satisfy the bond requirements suggested for octahedral Mn^{3+} by the Jahn-Teller theorem (Jahn and Teller 1937). Such distortion characterizes octahedral Mn^{3+} in several mineral structures. As described by Burns et al. (1994), Jahn-Teller-distorted $^{65}Mn^{3+}$ exhibits a strong correlation between the mean bond length and the dispersion of the individual values (Δ value). By using the relationship derived by Burns et al. (1994), in coralloite the distortion Δ is 0.0035 for M1 and 0.0039 for M2, that correspond to a calculated $\langle M1-O \rangle$ value of 2.017 Å and $\langle M2-O \rangle$ value of 2.020 Å, to be compared with the observed value of 2.014(7) Å for both sites. Therefore the distortions for M1 and M2 octahedra in coralloite are not significantly different from those expected for pure Mn^{3+} octahedral sites. Interestingly, also bermanite shows the behavior expected for pure $^{65}Mn^{3+}$ sites, whereas not-pure $^{65}Mn^{3+}$ distorted octahedra lie outside the relation of Burns et al. (1994). For instance, among minerals containing Mn^{3+} distorted octahedra, the hydrated phosphate erciticite (M1 site, Cooper et al. 2009) and the borates fredrikssonite (M4 site, Burns et al. 1994) and pinakiolite (M3 site, Moore and Araki 1974) have observed mean bond distances lying above the predicted values. These deviations have been ascribed to the presence of additional cations (as Fe^{3+}) in the Jahn-Teller-distorted Mn^{3+} octahedra (Burns et al. 1994; Cooper et al. 2009).

In coralloite ($P1$) the TO_4 tetrahedra, corner linked to the Mn^{3+} octahedral chains, occur as two independent atom sites (As1 and As2), whereas in bermanite ($P2_1$) these two sites are symmetrically equivalent (P sites; Kampf and Moore 1976). The AsO_4 tetrahedra show a fairly regular geometry: the mean bond lengths (1.683 and 1.673 Å for As1 and As2, respectively) indicate that they are fully As populated.

The adjacent $[^{65}Mn_3^{3+}(OH)_2(^{47}TO_4)_2]$ slabs in coralloite and bermanite are connected along **b** by means of isolated $Mn^{2+}O_2(H_2O)_4$ octahedra, which share the two O vertexes with two TO_4 tetrahedra belonging to two different $[Mn_3^{3+}(OH)_2(^{47}TO_4)_2]$ slabs (Fig. 3). In coralloite the Mn^{2+} octahedra (M3) show a mean bond length of 2.210 Å and the site is fully Mn^{2+} populated. However, the topological arrangement of $Mn^{2+}O_2(H_2O)_4$ octahedra in coralloite is different than in bermanite. Coralloite shows the Mn^{2+} octahedron with a *cis* configuration toward the position of the O species, whereas bermanite shows a *trans* Mn^{2+} octahedron (Kampf and Moore 1976). This difference is responsible for the absence of isomorphism between the two minerals. In fact, as shown in Figure 3, when the isolated Mn^{2+} octahedra change their configuration from *cis* to *trans*, the length of the **b** cell edge doubles and the symmetry changes. Actually, coralloite shows $b = 9.77(1)$ Å and its crystal structure is triclinic ($P1$), whereas bermanite shows $b = 19.25(1)$ Å and has a monoclinic structure ($P2_1$).

The presence of four H_2O molecules and two OH groups in coralloite allows extensive hydrogen-bond interactions in the crystal structure. However, also analyzing the final ΔF maps, the positions of H atoms remain undetermined. Identification of anion sites involved in H-bond interaction can be suggested on the basis of the analysis of the shortest O...O interatomic contacts, assumed as donor...acceptor interactions. A possible hydrogen-bond motif

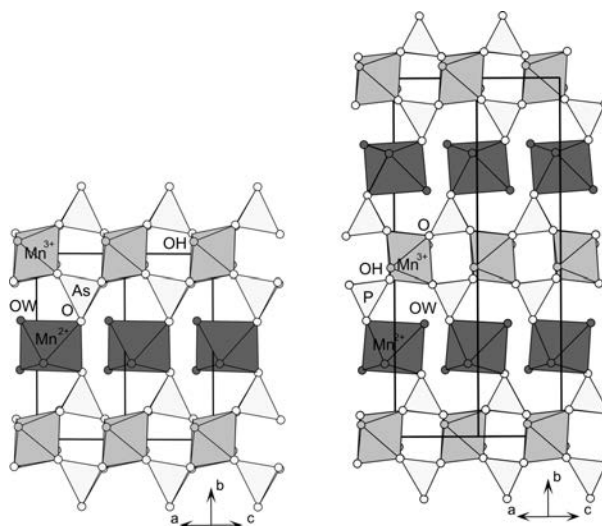


FIGURE 3. The connectivity between $[^{65}Mn_3^{3+}(OH)_2(^{47}XO_4)_2]$ sheets in coralloite ($X = As$, on the left) and bermanite ($X = P$, on the right) projected down $[010]$. The different lengths of the **b** cell edge and the different crystallographic symmetries (coralloite $P1$, bermanite $P2_1$) are due to the different configuration of the two O atoms of the Mn^{2+} octahedra (*cis* in coralloite, *trans* in bermanite).

for coralloite is summarized in Table 8. Possible acceptors of water proton result O1, O2, O6 (twice), O7 (twice), OH1, OH2, OW2, and OW3. This model has the advantage that the two unsaturated O species (O6 and O7, Table 6) act as acceptors of two hydrogen bonds. However, this is not the only scheme that can be recognized analyzing the structural features.

When the chemical composition of structural sites is not taken into account, coralloite, and bermanite structures are related by a polytypic relationship and features of this relation will be discussed below.

Optical and physical properties

Coralloite occurs as sub-millimetric red crystals, elongated on $[100]$ and flattened on (001) isolated or forming wisps up to 0.5–1 mm long. Neither the hardness nor the density could be measured because of the small size of crystals. The calculated density is 3.26 g/cm³.

Due to the small crystal size, only few optical properties of the mineral could be determined. Crystals are vitreous, translucent,

TABLE 8. Suggested donor...acceptor separations in coralloite

OW1...OH1	2.994(10)
OW1...O7	3.081(10)
OH1-OW1-O7	91.86(30)
OW2...O6	2.652(9)
OW2...O2	2.708(9)
O6-OW2-O2	81.86(29)
OW3...O7	2.695(8)
OW3...O1	2.921(9)
O7-OW3-O1	103.51(28)
OW4...OW2	2.777(10)
OW4...OW3	2.923(10)
OW2-OW4-OW3	101.67(37)
OH1...OH2	2.856(5)
OH2...O6	3.074(9)

and non-fluorescent; they are pleochroic, yellow along [100] and orange-red in directions normal to it. Extinction is parallel to the cleavage traces and elongation is negative. Birefringence is clearly visible in grains mounted in diiodomethane ($n = 1.74$), but it is not measurable. Crystals placed in diiodomethane show high relief in one direction and no relief when the polarizer is rotated by 90° . Thus we assume that the real mean refractive index should be close to 1.74. The Gladstone-Dale calculation gives a compatibility index of 0.036 (for $n = 1.74$ and the chemical formula derived by the structural study reported below), which is regarded as excellent (Mandarino 1981).

The mean refractive index has also been calculated using the method proposed by Korotkov and Atuchin (2008). According to these authors, the average error for oxide compounds is about 9%. The calculated mean refractive index of coralloite is 1.66(15) and it is close to the proposed value.

POLYTPIC RELATIONSHIP BETWEEN VARIOUS ARSENATE AND PHOSPHATE MINERALS

In addition to the two cases described above (coralloite and bermanite) the general formula $^{6[6]M^{2+}[6]M^{3+}}(TO_4)_2(OH)_2 \cdot 4H_2O$ characterizes other arsenate and phosphate minerals. All these species are related by polytypic relationship due to the different arrangement of the octahedral $M^{2+}O_2(H_2O)_4$, octahedral $M^{3+}O_4(OH)_2$, and tetrahedral TO_4 building blocks. In particular, both $M^{2+}O_2(H_2O)_4$ and $M^{3+}O_4(OH)_2$ octahedra can exhibit two different configurations (*trans* or *cis*) toward the position of the O and of the OH groups, respectively. Combinations of octahedra in different configurations lead to the formation of different crystal structures. As far as we know, only three of the possible combinations of the octahedral configurations are shown by mineral species.

The first case is that of *cis*- M^{2+} , two *trans*- M^{3+} , and isolated T polyhedral, which are interconnected to form a triclinic structure in which *trans*- M^{3+} octahedra form edge-connected chains, T- M^{3+} -T linkages generate slabs normal to **b**, *cis*- M^{2+} octahedra are isolated and the sequence (T- M^{3+} -T)- M^{2+} define the length of the

b axis. The resulting triclinic structure (*P1*) is that of coralloite: $^{6[6]Mn^{2+}[6]Mn^{3+}}(AsO_4)_2(OH)_2 \cdot 4H_2O$; $b = 9.8 \text{ \AA}$.

A second case is the linkage between a *trans*- M^{2+} , two *trans*- M^{3+} , and isolated T polyhedra, which leads to a monoclinic structure in which the T- M^{3+} -T polyhedral slab normal to **b** is the same as coralloite. The *trans*- M^{2+} octahedra are already isolated but in this case a double sequence (T- M^{3+} -T)- M^{2+} -(T- M^{3+} -T)- M^{2+} is required to obtain the unit of translation along the **b** direction. This monoclinic structure (*P2₁*) is that of bermanite: $^{6[6]Mn^{3+}}(PO_4)_2(OH)_2 \cdot 4H_2O$; $b = 19.4 \text{ \AA}$ (Kampf and Moore 1976).

The final case occurs when *trans*- M^{2+} , two *cis*- M^{3+} , and isolated T polyhedra are interconnected to form a monoclinic structure in which couples of edge-connected *cis*- M^{3+} octahedra are vertex-connected each other to form corrugated octahedral sheets. These octahedral sheets are connected to isolated T tetrahedra and generate T- M^{3+} -T slabs normal to **a** but different from those of coralloite and bermanite. These corrugated slabs are linked via isolated *trans*- M^{2+} octahedra, i.e., the same configuration of bermanite, but the structure implies only a single sequence (T- M^{3+} -T)- M^{2+} to define the length of the **a** axis. This monoclinic structure (*P2₁/c*) is represented by whitmoreite (Moore et al. 1974) and by all the minerals of the whitmoreite group: $^{6[6]M^{2+}[6]Fe^{3+}}(TO_4)_2(OH)_2 \cdot 4H_2O$; $a \sim 10 \text{ \AA}$ ($M^{2+} = Cu, Mn, Zn, Fe, Co$; T = As, P). Relations between the configuration of the octahedral building blocks and the resulting crystal structures are summarized in Table 9.

The main differences among structures with pairs of $^{6[6]M^{3+}}$ in the two different configurations are that the corrugated sheet allowed by *cis*- M^{3+} octahedra produces more regular polyhedra, with, in general, a less evident [4+2] octahedral coordination. The more regular *cis*-octahedra seem suitable for Fe^{3+} cations, that is the trivalent cation common for all the whitmoreite group minerals. On the contrary the geometrical distortion required by the Jahn-Teller effects of Mn^{3+} is better satisfied by chains of *trans*- M^{3+} octahedra. Actually, these chains have very similar features in the different crystal structures of coralloite and bermanite, both characterized by $^{6[6]Mn^{3+}}$ population. Interestingly, the hy-

TABLE 9. Possible crystal structures originating from the different configuration of bivalent and trivalent octahedra in arsenate and phosphate minerals

$^{6[6]M^{2+}}(H_2O)_4O_2$ configuration	<i>cis</i>	<i>trans</i>	<i>trans</i>	<i>trans</i>	<i>trans</i>	<i>trans</i>	<i>trans</i>	<i>trans</i>	<i>trans</i>
$^{6[6]M^{3+}}O_4(OH)_2$ configuration	<i>trans</i>	<i>trans</i>	<i>cis</i>	<i>cis</i>	<i>cis</i>	<i>cis</i>	<i>cis</i>	<i>cis</i>	<i>cis</i>
Mineral	coralloite	bermanite	arthurite	bendadaite	ojuelaite	cobaltarthurite	earlshannonite	kunatite	whitmoreite
Formula	$Mn^{2+}Mn^{3+}(AsO_4)_2(OH)_2 \cdot 4H_2O$	$Mn^{2+}Mn^{3+}(PO_4)_2(OH)_2 \cdot 4H_2O$	$Cu^{2+}Fe^{3+}(AsO_4)_2(OH)_2 \cdot 4H_2O$	$Fe^{2+}Fe^{3+}(AsO_4)_2(OH)_2 \cdot 4H_2O$	$Zn^{2+}Fe^{3+}(AsO_4)_2(OH)_2 \cdot 4H_2O$	$Co^{2+}Fe^{3+}(AsO_4)_2(OH)_2 \cdot 4H_2O$	$Mn^{2+}Fe^{3+}(PO_4)_2(OH)_2 \cdot 4H_2O$	$Cu^{2+}Fe^{3+}(PO_4)_2(OH)_2 \cdot 4H_2O$	$Fe^{2+}Fe^{3+}(PO_4)_2(OH)_2 \cdot 4H_2O$
System	tric	mon	mon	mon	mon	mon	mon	mon	mon
Space group	<i>P1</i>	<i>P2₁</i>	<i>P2₁/c</i>	<i>P2₁/c</i>	<i>P2₁/c</i>	<i>P2₁/c</i>	<i>P2₁/c</i>	<i>P2₁/c</i>	<i>P2₁/c</i>
<i>a</i> (Å)	5.583(1)	5.446(3)	10.189(2)	10.239	10.237(1)	10.264(1)	9.910(13)	9.863(10)	10.00(2)
<i>b</i> (Å)	9.766(1)	19.25(1)	9.649(2)	9.713	9.662(3)	9.703(1)	9.669(8)	9.661(6)	9.73(2)
<i>c</i> (Å)	5.546(1)	5.428(3)	5.598(1)	5.552	5.562(1)	5.571(1)	5.455(9)	5.476(6)	5.471(8)
α (°)	94.47(1)	–	–	–	–	–	–	–	–
β (°)	111.35(1)	110.29(4)	92.16(2)	94.11	94.36(1)	94.207(1)	93.95(9)	92.45(3)	93.8(1)
γ (°)	93.85(1)	–	–	–	–	–	–	–	–
<i>V</i> (Å ³)	279.26(6)	533.74	550.25	550.73	548.54	553.30(8)	521.46	521.3(3)	531.16
<i>Z</i>	1	2	2	2	2	2	2	2	2
Dana group	bermanite	bermanite	whitmoreite	whitmoreite	whitmoreite	whitmoreite	whitmoreite	whitmoreite	whitmoreite
Strunz group	08.DC.–†	08.DC.20	08.DC.15	08.DC.15	08.DC.15	08.DC.15	08.DC.15	08.DC.15	08.DC.15
References*	this work	2, 5, 8	3, 4	14	1, 6	7, 9, 13	12	10	11

Note: All the minerals above reported could be considered as phases of an hypothetical new arthurite supergroup.

* References: 1 = Cesbron et al. (1981); 2 = Cooper et al. (2009); 3 = Davis and Hey (1964); 4 = Keller and Hess (1978); 5 = Hurlbut (1936); 6 = Hughes et al. (1996); 7 = Kampf (2005); 8 = Kampf and Moore (1976); 9 = Jambor et al. (2002); 10 = Mills et al. (2008); 11 = Moore et al. (1974); 12 = Peacor et al. (1984); 13 = Raudsepp and Pani (2002); 14 = Kolitsch et al. (2010).

† Coralloite should be placed in a new coralloite group within the 08.DC family in the Strunz and Nickel classification rules.

drated phosphate mineral ercinite, $^{71}\text{Na}_2^{61}\text{Mn}_2^{3+}(\text{PO}_4)_2(\text{OH})_2 \cdot 4\text{H}_2\text{O}$ (Cooper et al. 2009), contains the same $^{61}\text{Mn}^{3+}$ and T building blocks of minerals described above. Also in this case, [4+2]-coordinated Mn^{3+} occurs as chains of *trans*- M^{3+} octahedral, which are connected to isolated T to form the T- M^{3+} -T slabs identical to those of coralloite and bermanite. In ercinite the slabs are normal to the *c* axis and interconnections among slabs are provided by pairs of corner sharing sevenfold-coordinated Na species, which substitute the octahedral $^{61}\text{M}^{2+}$ building block in this mineral structure.

CLASSIFICATION AND NOMENCLATURE

Coralloite shows structural similarities to bermanite, $\text{Mn}^{2+}\text{Mn}_2^{3+}(\text{PO}_4)_2(\text{OH})_2 \cdot 4\text{H}_2\text{O}$, and ercinite, $\text{Na}_2\text{Mn}_2^{3+}(\text{PO}_4)_2(\text{OH})_2 \cdot 4\text{H}_2\text{O}$. The three unit formulas can be expressed by using the following crystal chemical formulas: coralloite $^{61}\text{Mn}^{2+}(\text{H}_2\text{O})_4[^{61}\text{Mn}_2^{3+}(\text{OH})_2(\text{AsO}_4)_2]$, bermanite $^{61}\text{Mn}^{2+}(\text{H}_2\text{O})_4[^{61}\text{Mn}_2^{3+}(\text{OH})_2(\text{PO}_4)_2]$, ercinite $^{71}\text{Na}_2(\text{H}_2\text{O})_4[^{61}\text{Mn}_2^{3+}(\text{OH})_2(\text{PO}_4)_2]$, to emphasize that in all the three phases the topology of the $[^{61}\text{Mn}_2^{3+}(\text{OH})_2(\text{XO}_4)_2]$ (X = As or P) structural unit is the same. For this reason, coralloite can be placed in the 42.11.17 bermanite group, following the Dana classification (Gaines et al. 1997), together with bermanite and ercinite. However, bermanite and ercinite species belong to two different mineral groups following the Strunz and Nickel (2001) classification: ercinite is placed in the 08.DJ family because of the presence of the large Na cation, whereas bermanite has only medium-sized cations and is part of the 08.DC family. Also coralloite is a member of the 08.DC family but it cannot be placed in the same 08.DC.20 group containing bermanite because, as shown in this work, coralloite and bermanite have different crystal structure. Therefore, coralloite is the first member of a new still undefined Strunz and Nickel mineral group of the 08.DC family.

Coralloite and bermanite also show chemical similarities to phases of the whitmoreite group (Dana group 42.11.18, Strunz group 08.DC.15). In particular, coralloite, bermanite, and whitmoreite have crystal structures constituted by the same building blocks. However the *cis* or *trans* configuration shown by octahedral species is different and this makes their crystal structures different.

Recently, a revision of some minerals supergroups (e.g., Pasero et al. 2010) is underway and it is plausible to consider that a general revision will be applied to all known minerals groups in accordance with the newly approved standardization of mineral groups hierarchies suggested by Mills et al. (2009). The comparative study of coralloite, bermanite, and whitmoreite group minerals could provide some hints to a possible reevaluation of the hierarchies and supergroup relationships among these mineral species. In particular, all the minerals reported in Table 9 should be grouped in a new mineral supergroup (e.g., arthurite) not yet formally established, because they are constituted by the same structural building blocks: $\text{M}^{2+}\text{O}_2(\text{H}_2\text{O})_4$ isolated octahedra, $\text{M}^{3+}\text{O}_4(\text{OH})_2$ linked octahedra, TO_4 isolated tetrahedra; this mineral supergroup could be subdivided into two groups (e.g., arthurite and whitmoreite) based on the dominant tetrahedral species (As or P) and in further sub group hierarchies, based on the *cis* or *trans* configurations of the divalent and trivalent octahedra.

ACKNOWLEDGMENTS

We are very grateful to Günter Blass for the electron microprobe analyses. We are indebted also to Olaf Medenbach for the several attempts he made to measure the indices of refractions of this new mineral phase although it was a very small crystal; unfortunately too small! The authors thank Alessandro Pozzi, a local mineral collector, that first found the coralloite and provided us the specimens for this study. Sincere thanks are due to the referees Kimberly Tait and Mark Cooper and to the Associated Editor Andrew McDonald for their suggestions. A.M.C. and M.B. are supported by funds of two different MIUR-PRIN 2009 projects and by the University of Pavia.

REFERENCES CITED

- Altomare, A., Burla, M.C., Camalli, M., Cascarano, G.L., Giacovazzo, C., Guagliardi, A., Moliterni, A.G.G., Polidori, G., and Spagna, R. (1999) SIR97: a new tool for crystal structure determination and refinement. *Journal of Applied Crystallography*, 32, 115–119.
- Antofilli, M., Borgo, E., and Palenzona, A. (1983) I nostri minerali. *Geologia e mineralogia in Liguria*. SAGEP Editrice, Genova, 295 pp (in Italian).
- Balestra, C., Kolitsch, U., Blass, G., Callegari, A.M., Boiocchi, M., Armellino, G., Ciriotti, M.E., Ambrino, P., and Bracco, R. (2009) Mineralogia figure 2007–2008: novità caratterizzate dal Servizio UK dell'AMI. *Micro (UK report)*, 1/2009, 78–99 (in Italian).
- Basso, R., Lucchetti, G., and Palenzona, A. (1991) Gravegliaite, $\text{MnSO}_4 \cdot 3\text{H}_2\text{O}$, a new mineral from Val Graveglia, (Northern Apennines, Italy). *Zeitschrift für Kristallographie*, 197, 97–106.
- Basso, R., Lucchetti, G., Zefiro, L., and Palenzona, A. (1992) Reppiaite, $\text{Mn}_2(\text{OH})_4(\text{VO}_4)_2$, a new mineral from Val Graveglia (Northern Apennines, Italy). *Zeitschrift für Kristallographie*, 201, 223–234.
- Basso, R., Carbone, C., and Palenzona, A. (2008) Cassagnaite, a new V-bearing silicate mineral from the Cassagna mine, northern Apennines, Italy. *European Journal of Mineralogy*, 20, 95–100.
- Bersani, D., Balestra, C., Kolitsch, U., Blass, G., Ciriotti, M.E., and Ambrino, P. (2009) La spettroscopia Raman a supporto della mineralogia sistematica ligure. *Micro (UK report)*, 2/2009, 112–117 (in Italian).
- Bonatti, E., Zerbi, M., Kay, R., and Rydell, H. (1976) Metalliferous deposits from the Apennine ophiolites: Mesozoic equivalents of modern deposits from oceanic spreading centers. *Bulletin of the Geological Society of America*, 87, 83–94.
- Boni, A. (1986) Carta geologica schematica dell'Appennino Settentrionale. *Atti dell'Istituto di Geologia dell'Università di Pavia*, 12 (in Italian).
- Brese, N.E. and O'Keeffe, M. (1991) Bond-valence parameters for solids. *Acta Crystallographica*, B47, 192–197.
- Brown, I.D. and Altermatt, D. (1985) Bond-valence parameters obtained from a systematic analysis of the inorganic crystal structure database. *Acta Crystallographica*, B41, 244–247.
- Bruker (2003) SAINT Software Reference Manual. Version 6. Bruker AXS Inc., Madison, Wisconsin.
- Burns, P.C., Cooper, M., and Hawthorne, F.C. (1994) Jahn-Teller distorted Mn^{3+}O_6 octahedra in fredrikssonite, the fourth polymorph of $\text{Mg}_2\text{Mn}^{3+}(\text{BO}_3)_2$. *The Canadian Mineralogist*, 32, 397–403.
- Busing, W.R., Martin, K.O., and Levy, H.A. (1962) ORFLS. Report ORNL-TM-305. Oak Ridge National Lab, Tennessee.
- Cabella, R., Lucchetti, G., and Marescotti, P. (1998) Mn-ores from Eastern Ligurian ophiolitic sequences ("Diaspri di Monte Alpe" Formation, Northern Apennines, Italy). *Research Trends—Trends in Mineralogy*, 2, 1–17.
- Cabella, R., Basso, R., Lucchetti, G., and Palenzona, A. (2000) Geigerite from Mt. Nero manganese mine, Northern Apennines, La Spezia, Italy. *Neues Jahrbuch für Mineralogie Monatshefte*, 12, 570–576.
- Callegari, A.M., Boiocchi, M., Ciriotti, M.E., and Balestra, C. (2010) Coralloite, IMA 2010-012. *Mineralogical Magazine*, 74, 577–579.
- Cesbron, F., Romero S.M., and Williams, S.A. (1981) La mapimite et l'ojuelaite, deux nouveaux arseniates hydratés de zinc et de fer de la mine Ojuela, Mapimi, Mexique. *Bulletin de Minéralogie*, 104, 582–586 (in French).
- Cooper, M.A., Hawthorne, F.C., and Černý, P. (2009) The crystal structure of ercinite, $\text{Na}_2(\text{H}_2\text{O})_4[\text{Mn}_2^{3+}(\text{OH})_2(\text{PO}_4)_2]$, and its relation to bermanite, $\text{Mn}^{2+}(\text{H}_2\text{O})_4[\text{Mn}_2^{3+}(\text{OH})_2(\text{PO}_4)_2]$. *Canadian Mineralogist*, 47, 173–180.
- Cortesogno, L., Lucchetti, G., and Penco, A.M. (1979) Le mineralizzazioni a manganese nei diaspri delle ophioliti liguri: mineralogia e genesi. *Rendiconti Società Italiana di Mineralogia e Petrologia*, 35, 151–197 (in Italian).
- Davis, R.J. and Hey, M.H. (1964) Arthurite, a new copper-iron arsenate from Cornwall. *Mineralogical Magazine*, 33, 937–941.
- Dunn, P.J., Peacor, D.R., Leavens, P.B., and Simmons, W.B. (1982) Jarosewichtite and a related phase: basic manganese arsenates of the chlorophoenicite group from Franklin, New Jersey. *American Mineralogist*, 67, 1043–1047.
- Gaines, R.V., Skinner, H.C., Foord, E.E., Mason, B., and Rosenzweig, A. (1997) *Dana's New Mineralogy*. Wiley, New York.
- Garuti, G., Bartoli, O., Scacchetti, M., and Zaccarini, F. (2008) Geological setting

- and structural styles of Volcanic Massive Sulfide deposits in the northern Apennines (Italy): evidence for seafloor and sub-seafloor hydrothermal activity in unconventional ophiolites of the Mesozoic Tethys. *Boletín de la Sociedad Geológica Mexicana*, 60, 121–145.
- Guelfi, F. and Orlandi, P. (1987) Brevissime segnalazioni da diverse località mineralogiche italiane. *Rivista Mineralogica Italiana*, 1/1987, 51–54 (in Italian).
- Hughes, J.M., Bloodaxe, E.S., and Kobel, K.D. (1996) The atomic arrangement of ojuelaite, $\text{ZnFe}_2^{3+}(\text{AsO}_4)_2(\text{OH})_2 \cdot 4\text{H}_2\text{O}$. *Mineralogical Magazine*, 60, 519–521.
- Hurlbut, C.S. Jr. (1936) A new phosphate, bermanite, occurring with triplite in Arizona. *American Mineralogist*, 21, 656–661.
- Hurlbut, C.S. Jr. and Aristarain, L.F. (1968) Bermanite and its occurrences in Córdoba, Argentina. *American Mineralogist*, 53, 416–431.
- Issel, A. (1892) *Liguria geologica e preistorica*, vol. 1 and vol 2. Donath ed., Genova.
- Jahn, H.A. and Teller, E. (1937) Stability of polyatomic molecules in degenerate electronic states. I. Orbital degeneracy. *Proceeding of the Royal Society, A*, 161, 220–235.
- Jambor, J.L., Viñals, J., Groat, L.A., and Raudsepp, M. (2002) Cobaltarthurite, $\text{Co}^{2+}\text{Fe}_3^{3+}(\text{AsO}_4)_2(\text{OH})_2 \cdot 4\text{H}_2\text{O}$, a new member of the arthurite group. *Canadian Mineralogist*, 40, 725–732.
- Kampf, A.R. (2005) The crystal structure of cobaltarthurite from the Bou Azzer District, Morocco: the location of hydrogen atoms in the arthurite structure type. *Canadian Mineralogist*, 43, 1387–1391.
- Kampf, A.R. and Moore, P.B. (1976) The crystal structure of bermanite, a hydrated manganese phosphate. *American Mineralogist*, 61, 1241–1248.
- Keller, P. and Hess, H. (1978) Die Kristallstruktur von Arthurit, $\text{CuFe}_2^{3+}[(\text{H}_2\text{O})_4(\text{OH})_2](\text{AsO}_4)_2$. *Neues Jahrbuch für Mineralogie Abhandlungen*, 133, 291–302 (in German).
- Kolitsch, U. (2001) Redetermination of the mixed-valence manganese arsenate flinkite, $\text{Mn}^{II}_2\text{Mn}^{III}(\text{OH})_4(\text{AsO}_4)_2$. *Acta Crystallographica*, E57, i115–i118.
- Kolitsch, U., Atencio, D., Chukanov, N.V., Zubkova, N.V., Menezes Filho, L.A.D., Coutinho, J.M.V.W.D., Birch, J., Schlüter, D., Pohl, A., and others. (2010) Bendadaite, a new iron arsenate mineral of the arthurite group. *Mineralogical Magazine*, 74, 469–486.
- Korotkov, A.S. and Atuchin, V.V. (2008) Prediction of refractive index of inorganic compound by chemical formula. *Optics communications*, 281, 2132–2138.
- Mandarino, J.A. (1981) The Gladstone Dale relationship, IV. The compatibility concept and its application. *Canadian Mineralogist*, 19, 441–450.
- Marchesini, M. (1999) Tronchi silicizzati: associazioni a rame, arsenico e vanadio. *Rivista Mineralogica Italiana*, 2/1999, 116–121 (in Italian).
- Marchesini, M. and Palenzona, A. (1997) Il giacimento manganesifero di Monte Nero (Rocchetta Vara, La Spezia). *Rivista Mineralogica Italiana*, 1/1997, 51–55.
- Marroni, M., Molli, G., Montanini, A., Ottria, G., Pandolfi, L., and Tribuzio, R. (2002) The External Ligurian units (Northern Apennine, Italy): from rifting to convergence of a fossil ocean-continent transition zone. *Ophioliti*, 27, 119–131.
- Mills, S.J., Kolitsch, U., Birch, W.D., and Sejkora, J. (2008) Kunitite, $\text{CuFe}_2(\text{PO}_4)_2(\text{OH})_2 \cdot 4\text{H}_2\text{O}$, a new member of the whitmoreite group, from Lake Boga, Victoria, Australia. *Australian Journal of Mineralogy*, 14, 3–12.
- Mills, S.J., Hatert, F., Nickel, E.H., and Ferraris, G. (2009) The standardisation of mineral group hierarchies: application to recent nomenclature proposals. *European Journal of Mineralogy*, 21, 1073–1080.
- Mognol, A. (1924) Il giacimento manganesifero di Monte Nero, Rocchetta Vara. *Memorie dell'Accademia Lunigianese di scienze lettere ed arti "Giovanni Capellini"*, 5, 119–123 (in Italian).
- Moore, P.B. and Araki, T. (1974) Pinakiolite, $\text{Mg}_2\text{Mn}^{3+}\text{O}_2[\text{BO}_3]$; warwickite, $\text{Mg}(\text{Mg}_{0.5}\text{Ti}_{0.5})\text{O}[\text{BO}_3]$; wightmanite, $\text{Mg}_5(\text{O})(\text{OH})_5[\text{BO}_3] \cdot n\text{H}_2\text{O}$: Crystal chemistry of complex 3 Å wallpaper structures. *American Mineralogist*, 59, 985–1004.
- Moore, P.B., Kampf, A.R., and Irving, A.J. (1974) Whitmoreite, $\text{Fe}^{2+}\text{Fe}^{3+}(\text{OH})_2(\text{H}_2\text{O})_4[\text{PO}_4]_2$, a new species: its description and atomic arrangement. *American Mineralogist*, 59, 900–905.
- Palenzona, A. and Martinelli, A. (2009) Cassagnaite una nuova specie vanadinifera dalla Val Graveglia, Genova. *Rivista Mineralogica Italiana*, 4/2009, 268–270 (in Italian).
- Palenzona, A., Balestra, C., and Marchesini, M. (2002) La geigerite della miniera di Monte Nero (Rocchetta Vara, La Spezia). *Rivista Mineralogica Italiana*, 2/2002, 75–76 (in Italian).
- Pasero, M., Kampf, A.R., Ferraris, C., Pekov, I.V., Rakovan, J., and White, T.J. (2010) Nomenclature of the apatite supergroup minerals. *European Journal of Mineralogy*, 22, 163–179.
- Passarino, G. (2009) L'inesite della Miniera di Monte Nero, Rocchetta Vara, Val di Vara, La Spezia. *Rivista Mineralogica Italiana*, 4, 260–262 (in Italian).
- Peacor, D.R., Dunn, P.J., and Simmons, W.B. (1984) Earlshannonite, the Mn analogue of whitmoreite, from North Carolina. *Canadian Mineralogist*, 22, 471–474.
- Raudsepp, M. and Pani, E. (2002) The crystal structure of cobaltarthurite, $\text{Co}^{2+}\text{Fe}_3^{3+}(\text{AsO}_4)_2(\text{OH})_2 \cdot 4\text{H}_2\text{O}$, a Rietveld refinement. *Canadian Mineralogist*, 40, 733–737.
- Roth, P. and Meisser, N. (2011) I minerali dell'Alpe Tanatz Passo dello Spluga (Grigioni, Svizzera). *Rivista Mineralogica Italiana*, 2, 90–98 (in Italian).
- Sheldrick, G.M. (1996) SADABS. University of Göttingen, Germany.
- Strunz, H. and Nickel, E.H. (2001) *Strunz Mineralogical Tables. Chemical-structural mineral classification system*, 9th ed. Schweizerbart, Stuttgart, Germany.
- Viviani, D. (1807) Voyage dans les Apennins de la ci-devant Ligurie pour servir d'introduction à l'histoire naturelle de ce pays. Giossi Editor, Genova, 28 p. (in French).

MANUSCRIPT RECEIVED MAY 10, 2011

MANUSCRIPT ACCEPTED NOVEMBER 21, 2011

MANUSCRIPT HANDLED BY ANDREW McDONALD